



# Covalent Amine Tethering on Ketone Modified Porous Organic Polymers for Enhanced CO<sub>2</sub> Capture

Perman Jorayev,<sup>[a, e]</sup> Intizar Tashov,<sup>[b]</sup> Vepa Rozyyev,<sup>[a, f]</sup> Thien S. Nguyen,<sup>[a]</sup> Nesibe A. Dogan,<sup>[b]</sup> and Cafer T. Yavuz<sup>\*[a, b, c, d]</sup>

Effective removal of excess greenhouse gas CO<sub>2</sub> necessitates new adsorbents that can overcome the shortcomings of the current capture methods. To achieve that, porous materials are often modified post-synthetically with reactive amine functionalities but suffer from significant surface area losses. Herein, we report a successful amine post-functionalization of a highly porous covalent organic polymer, COP-130, without losing much porosity. By varying the amine substituents, we recorded

a remarkable increase in CO<sub>2</sub> uptake and selectivity. Ketone functionality, a rarely accessible functional group for porous polymers, was inserted prior to amination and led to covalent tethering of amines. Interestingly, aminated polymers demonstrated relatively low heats of adsorption, which is useful for the rapid recyclability of materials, due to the formation of suspected intramolecular hydrogen bonding.

## Introduction

Greenhouse gases that absorb sunlight and release it slowly over time keep the average temperature on Earth above freezing.<sup>[1]</sup> However, a sharp increase in greenhouse gas levels over the past century due to the industries that process a high volume of fossil fuels led to significant temperature rise on Earth, which is known as global warming. Carbon dioxide (CO<sub>2</sub>) is considered as one of the main heat-trapping greenhouse gases. Current reports indicate that the atmospheric amount of CO<sub>2</sub> has reached 412 ppm<sup>[2]</sup> and is estimated to increase as high as 600–1500 ppm by 2030 if not prevented.<sup>[3]</sup> It has been known that high CO<sub>2</sub> levels intensify catastrophic events such as heatwaves, pollution, and ocean acidification. A promising alternative to fossil fuel consumption to meet the energy

demand is renewable energy such as solar, wind, and hydro-power. The renewable energy technologies, however, need further research and development to be widely implemented, indicating that fossil fuel usage is unlikely to be halted soon. In the interim, this necessitates technologies that can efficiently capture excess CO<sub>2</sub> and possibly decrease its concentration in the atmosphere. Various methods were used to address the issue such as the alkanolamine solutions (also known as “scrubbing”), among which monoethanolamine (MEA) is the benchmark absorbent. MEA has major disadvantages such as degradation, corrosiveness, toxic nature, and irreversible chemical binding of CO<sub>2</sub> that makes the regeneration of the material very costly.<sup>[4]</sup> Therefore, the discovery of new chemistries and materials is critical to come up with an efficient way of capturing CO<sub>2</sub>.<sup>[5]</sup>

Solid sorbents have shown great potential in overcoming the shortcomings of MEA.<sup>[5]</sup> They have high durability against harsh conditions such as high pressure and temperature, are not as toxic, and show tunable chemical properties that enable to alter the material's gas selectivity, capture capacity, and binding energy.<sup>[4b,d,5,6]</sup> Various solid sorbents such as petroleum and biomass-based activated carbon,<sup>[7]</sup> metal organic frameworks (MOFs),<sup>[4a,8]</sup> covalent organic polymers (COPs),<sup>[4c,9]</sup> and other porous materials have been discovered and investigated for CO<sub>2</sub> separation and capture in fossil fuel pre-combustion and post-combustion conditions. Porous materials are indeed promising in many areas not just CO<sub>2</sub> capture,<sup>[4c,9b,10]</sup> but also in methane storage,<sup>[11]</sup> water treatment,<sup>[12]</sup> and catalysis.<sup>[13a]</sup> Although various adsorbents have been developed with varying porosity, they have limited use in CO<sub>2</sub> scrubbing due to the lack of CO<sub>2</sub>-philic functionalities. One effective strategy to improve porous materials' CO<sub>2</sub> capture is to introduce amine functionality during post-modification.<sup>[4c,13]</sup> However, any kind of treatment performed on porous materials, including post-modification, results in significant surface area and pore volume loss, which in return has a negative impact on gas adsorption capacity.<sup>[5,9c]</sup> Loss of a large portion of surface area in porous

[a] P. Jorayev, V. Rozyyev, Dr. T. S. Nguyen, Prof. C. T. Yavuz  
Graduate School of Energy, Environment, Water and Sustainability (EEWS)  
Korea Advanced Institute of Science and Technology (KAIST)  
291 Daehak-ro, Yuseong-gu, Daejeon, 34141 (Korea)  
E-mail: yavuz@kaist.ac.kr


[b] I. Tashov, Dr. N. A. Dogan, Prof. C. T. Yavuz  
Department of Chemical and Biomolecular Engineering KAIST  
291 Daehak-ro, Yuseong-gu, Daejeon, 34141 (Korea)


[c] Prof. C. T. Yavuz  
Department of Chemistry KAIST  
291 Daehak-ro, Yuseong-gu, Daejeon, 34141 (Korea)

[d] Prof. C. T. Yavuz  
KAIST Institute for the NanoCentury KAIST  
291 Daehak-ro, Yuseong-gu, Daejeon, 34141 (Korea)

[e] P. Jorayev  
Department of Chemical Engineering and Biotechnology  
University of Cambridge  
Cambridge CB3 0AS (UK)

[f] V. Rozyyev  
Pritzker School of Molecular Engineering  
University of Chicago  
Chicago, IL 60637 (USA)

 Supporting information for this article is available on the WWW under <https://doi.org/10.1002/cssc.202002190>

 This publication is part of a Special Issue entitled “Green Carbon Science: CO<sub>2</sub> Capture and Conversion”. Please visit the issue at <http://doi.org/10.1002/cssc.v13.23>.

polymers has been a widespread issue with no straightforward solutions. Therefore, during post modification the use of non-invasive chemicals that preserve the surface area and functionality is fundamentally important.

Although scarce, amine attachment to porous polymers has previously been reported in the literature.<sup>[14,15]</sup> For example, Eddaoudi incorporated –CHO group to anchor ethylenediamine (EDA) on Porous Organic Polymers (POPs).<sup>[9a]</sup> Zhou group modified Porous Polymer Networks (PPNs) to introduce –CH<sub>2</sub>Cl units as tethering spots for diethylenetriamine (DETA), triethylenetetramine (TETA), and EDA.<sup>[16]</sup> We have also reported a –CH<sub>2</sub>Cl route for amine tethering in COPs and discovered a unique wrapping mechanism in CO<sub>2</sub> capture.<sup>[4c]</sup> Despite the potential in carbonyl modification and subsequent amine attachment, ketones have rarely been introduced as anchor points in porous polymers, either during the synthesis or through post-modification. Herein we demonstrate a successful modification of a highly porous covalent organic polymer, named COP-130, with chloroacetyl chloride molecules without significant loss of surface area. One significant advantage of acyl chloride functionalization is that it introduces two different functionalities at once: alkyl chloride and ketone. This further allows to perform modifications in confined spaces of porous materials for various applications, one of which is post-combustion CO<sub>2</sub> capture by amine functionalization. To test our materials for CO<sub>2</sub> capture, amines of ranging sizes were then attached to ketone groups by a favorable Schiff base approach

and nucleophilic substitution with chlorine atoms (via S<sub>N</sub>2 mechanism). CO<sub>2</sub> uptake of the resulting modified polymers noticeably increased, where the CO<sub>2</sub>/N<sub>2</sub> selectivity reached 105.

## Results and Discussion

The porous polymers have wide range of features and drawbacks that distinguish them from each other. For example, PAFs show record high surface areas but are expensive and require air-free synthetic conditions. In this work, we used hyper-crosslinking approach, a decades old method for making robust C–C bonded networks. COP-130 synthesis method utilized solvent linking procedure that we recently reported to make inexpensive porous polymers with robust structure to withstand Friedel-Crafts acylation.<sup>[11]</sup> In a typical run, 1,3,5-triphenylbenzene (1 g, 3.26 mmol) and dry solid AlCl<sub>3</sub> (1.31 g, 9.82 mmol) were placed in a 50 mL round bottom flask (RBF) followed by dropwise injection of excess amount of the linker solvent CH<sub>2</sub>Cl<sub>2</sub> (20 mL) and the mixture was heated to 38 °C with rigorous stirring for 24 h under inert atmosphere (Figure 1a). The precipitate was filtered, sonicated in 1 M HCl (in methanol) for an hour, and washed in a Soxhlet extractor with 100 mL chloroform and 100 mL methanol for 24 h followed by vacuum drying at 120 °C for 12 h.

Post-modification of COP-130 involves Friedel-Crafts acylation with chloroacetyl chloride (abbreviated as COP-130-Ac)

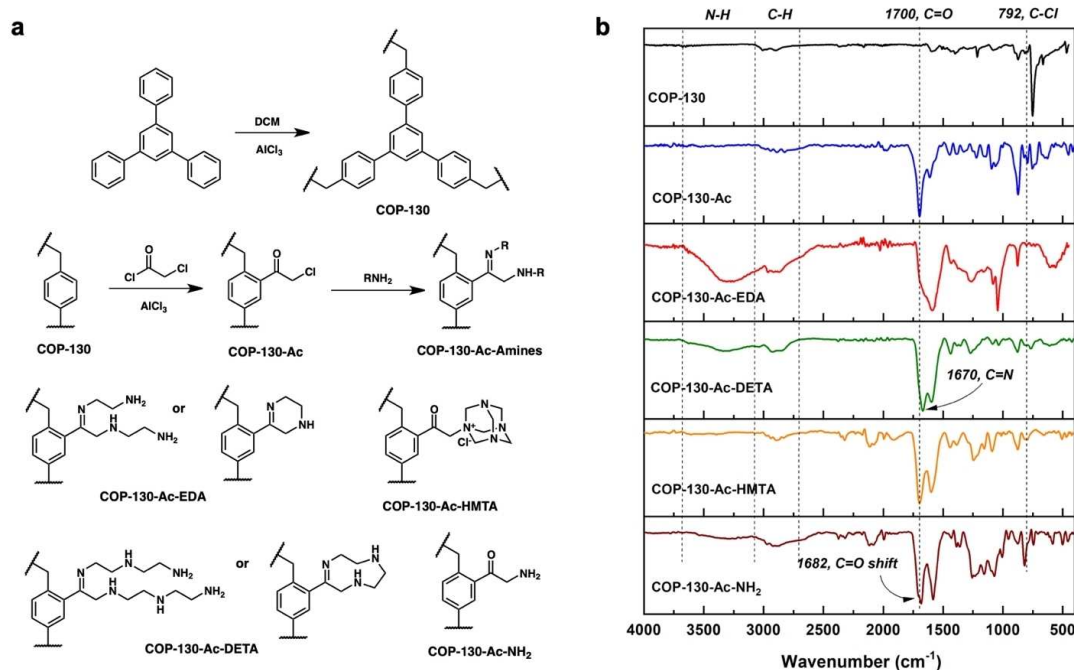


**Figure 1.** a) Synthesis of COP-130, COP-130-Acylated (COP-130-Ac), and COP-130-Ac-Amines. b) Structural analysis of COP-130, COP-130-Ac, and COP-130-Ac-Amines using FTIR spectroscopy.

followed by Schiff base amination and nucleophilic amine substitution. The main advantage of our approach is the dual introduction of an acyl and methylene chloride groups before attaching amine moiety in the porous material. This leads to double functionalization potential in a single step. 1 g of COP-130 and 2 g of  $\text{AlCl}_3$  were placed in a 50 mL RBF followed by a dropwise injection of 20 mL chloroacetyl chloride (in excess amount) and the mixture was heated to  $60^\circ\text{C}$  with stirring for 24 h and open to air. The product was filtered, sonicated in 1 M HCl (in methanol) for an hour, and washed in a Soxhlet extractor with 100 mL chloroform and 100 mL methanol mixture for 24 h followed by vacuum drying at  $110^\circ\text{C}$  for 12 h.

Amination of COP-130-Ac (abbreviated as COP-130-Ac-Amine) was performed by the addition of 0.25 g of COP-130-Ac into a 50 mL RBF followed by dropwise injection of 20 mL EDA (in excess amount) and the mixture was heated to  $80^\circ\text{C}$  with stirring for 24 h and open to air. The product was filtered, washed with distilled water, methanol, chloroform (100 mL each) and dried in a vacuum oven at  $110^\circ\text{C}$  for 12 h. DETA treatment of COP-130-Ac was also performed in the same way as EDA. 2 g of solid hexamethylenetetramine (HMTA) was dissolved in 20 mL ethanol and reacted with 0.25 g COP-130-Ac in the same way as EDA. HMTA rings are then transformed into primary amine through concentrated HCl (1 M in 20 mL ethanol) treatment for 24 h. The resultant product is collected, washed, and dried as the rest of the amines. See Supporting Information for the details of the synthetic methods (Scheme S1).

The addition of carbonyl units prompted us to monitor FTIR spectra first, since the progression of modification can be easily tracked. The FTIR spectra of COP-130 (Figure 1b) demonstrates a broad aliphatic peak in the range of  $2850\text{--}3000\text{ cm}^{-1}$  that persists throughout all the other structures as well, small C–Cl peak at  $792\text{ cm}^{-1}$ ,<sup>[18]</sup> and a sharp peak at  $750\text{ cm}^{-1}$ <sup>[19]</sup> that arises from the linker orientation on the aromatic ring. Acylated polymer shows a strong carbonyl peak appearance at

$1700\text{ cm}^{-1}$ <sup>[18]</sup> and a noticeable increase in C–Cl peak intensity. Further amination results in a significant decrease in C–Cl peak intensity, which suggests the successful substitution of Cl atoms by amines. The broad peak at  $3250\text{--}3500\text{ cm}^{-1}$  emerges from primary and secondary amine stretching and indicates the presence of intramolecular hydrogen bonding in amine groups.<sup>[20]</sup> It is known that hydrogen bonding makes the peaks significantly broader, which is probably why the amine stretching peaks are not as sharp.<sup>[17]</sup> All of the amine structures show a strong peak at  $1580\text{--}1600\text{ cm}^{-1}$  that corresponds to N–H bending from primary amine<sup>[21]</sup> (secondary amines give relatively weaker N–H bending peak) and aromatic C=C stretching.<sup>[19]</sup> EDA and DETA attached polymers show loss of the carbonyl peak. COP-130-Ac-DETA has a strong imine peak at  $1670\text{ cm}^{-1}$  that is not observed in COP-130-Ac-EDA. One plausible explanation would be the small size of EDA molecules that allow a second amine addition to its early imine form to form aminal (which also includes the possibility of cyclization of the already attached EDA molecule) as shown in Scheme S2.<sup>[21,22]</sup> This phenomenon is less likely to occur in DETA as its bulky size might hinder the addition of another amine molecule. COP-130-Ac-HMTA has a strong peak at  $1599\text{ cm}^{-1}$  that should not be confused with primary N–H bending as it corresponds to aromatic C=C stretch. COP-130-Ac-NH<sub>2</sub> develops a broad primary N–H stretch at  $745\text{ cm}^{-1}$  (that was less in intensity in other amines) from primary amine and a small shift (ca.  $18\text{ cm}^{-1}$ ) in carbonyl group ( $1682\text{ cm}^{-1}$ ) probably due to the formation of a favorable five-membered ring that includes an intramolecular hydrogen bonding between the carbonyl and amine groups (N–H–O).<sup>[23]</sup>

For gas uptake, the porosity of a material is equally important as its chemical composition. The BET surface area of COP-130 is found to be  $1813\text{ m}^2/\text{g}$  with the polymer being micro- and mesoporous as can be seen from its  $\text{N}_2$  (77 K) isotherm, which shows the characteristics of an isotherm type I with slight features of a type IV (Figure 2). Non-local density

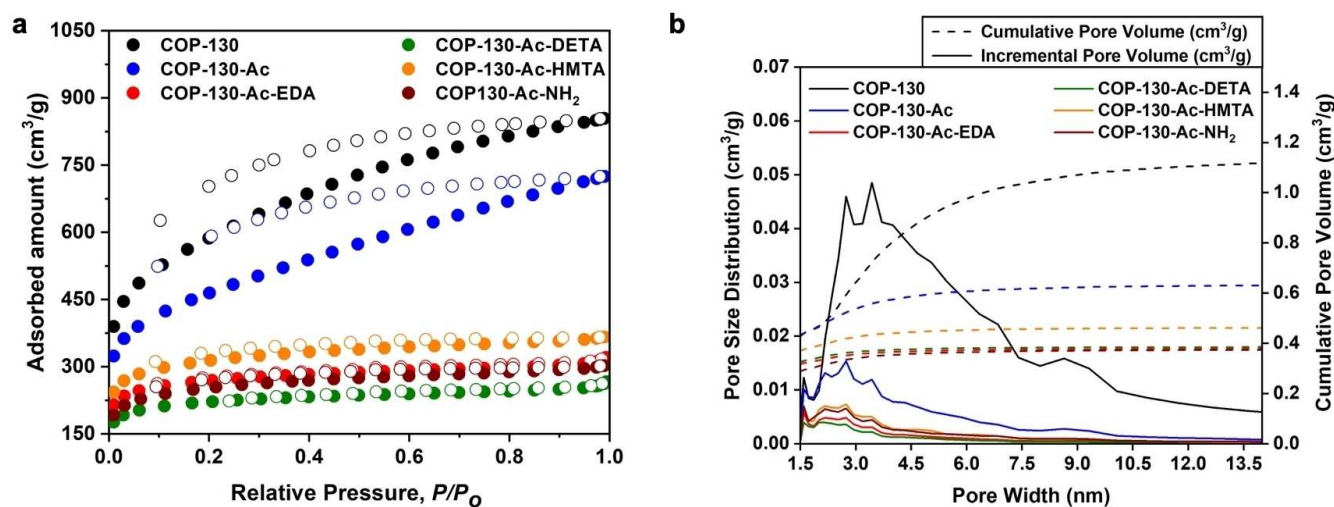


Figure 2. a) BET surface area isotherms of COP-130, COP-130-Ac, and COP-130-Ac-Amines using  $\text{N}_2$  gas at 77 K. b) Pore size distribution and cumulative pore volume of COP-130, COP-130-Ac, and COP-130-Ac-Amines.

functional theory (NLDFT) Carbon-Slit Pores kernel was utilized in pore size distribution calculations (details are explained in the Supporting Information). A closer look at the pore size distribution (PSD) of COP-130 shows that the polymer possesses 1.15 cm<sup>3</sup>/g total pore volume and the average pore size diameter of 3.05 nm supports that the mesopores are slightly dominating over the micropores (Table 1). BET (micro) is the surface area of the pores with less than 2 nm pore size diameter. On the other hand, the total BET surface area includes all the pores of the material. More than 80% of the original surface area is preserved after acylation of the polymer, which is equivalent to 1461 m<sup>2</sup>/g surface area and 0.64 cm<sup>3</sup>/g total pore volume. The micropore surface area shows twice an increase from 457 m<sup>2</sup>/g for COP-130 to 918 m<sup>2</sup>/g for COP-130-Ac.

Compared to the similar reported post-functionalization studies, COP-130 preserves more fraction of the surface area and possesses two functional groups - carbonyl and alkyl chloride inside the pores. For example, in Zhou et al.'s work<sup>[24]</sup> on introduction of -CH<sub>2</sub>Cl to PAFs, the surface area dramatically decreases from 4023 m<sup>2</sup>/g to 1740 m<sup>2</sup>/g (2.3× or 56.7%). In Lau et al.'s work,<sup>[25]</sup> p-DCX was changed to NH<sub>2</sub>-p-DCX as the result of amine functionalization. During the process, surface area decreases from 1330 m<sup>2</sup>/g to 767 m<sup>2</sup>/g (1.7× or 42.3%). In our work, we demonstrate that the surface area in the first functionalization step decreases from 1813 m<sup>2</sup>/g to 1461 m<sup>2</sup>/g (1.2× or 19.4%). One reason for the significant surface area preservation in COP-130 (>80%) and an increase in micropore surface area is believed to be COP-130's predominantly mesoporous structure that allowed the functionalization of pores without blocking them. Another reason might be the internal cross-linking of phenyl rings by chloroacetyl chloride molecules, a phenomenon that was observed by Liu et al. (2017).<sup>[26]</sup> Further amine treatment left the polymer with the surface area of 1002 m<sup>2</sup>/g for COP-130-Ac-EDA, 827 m<sup>2</sup>/g for -DETA, and 937 m<sup>2</sup>/g for -NH<sub>2</sub> (-HMTA possesses 1166 m<sup>2</sup>/g). Nitrogen isotherm of amine attached polymers quickly reach their respective saturation pressures that coupled with around 2 nm average pore size diameter indicate that the polymers became almost completely microporous due to pore filling.

Rouquerol plots and BET range plots for calculating the BET surface area can be found in Figure S2.

Elemental analyses of the materials are also in correspondence with successful post-modification (Table S1). The nitrogen content of aminated polymers comes short of the theoretically calculated values and the difference increases in relation to an amine molecule size, which is probably due to large amine molecules being unable to reach the innermost oxygen and chlorine atoms. The aluminum content of COP-130 and COP-130-Ac were computed from the residual mass values that were obtained from the TGA analyses (Figure S3) and found to be close to 0.00% and 0.82%, respectively.

COP-130, being a highly porous material (1813 m<sup>2</sup>/g surface area), adsorbs 3.84 mmol/g of CO<sub>2</sub> at 273 K that decreases with increase in temperature, which is an expected phenomenon (Figure 3).<sup>[5]</sup> Further modification with chloroacetyl chloride increases the uptake by 19% reaching up to 4.58 mmol/g even though COP-130-Ac possesses a 20% lower surface area than its predecessor. We believe, the introduction of new functional groups and improved microporosity makes up for the surface area difference. Compared to the parent COP-130's uptake, EDA, DETA, and NH<sub>2</sub> insertion results in 45%, 54%, and 48% surface area losses, respectively. Despite the loss of half of the original surface area, -EDA shows 4.95 mmol/g (29% increase compared to the starting material), -DETA reaches 3.72 mmol/g (3% decrease), and -NH<sub>2</sub> has 4.37 mmol/g (14% increase) of CO<sub>2</sub> uptake, all of which are comparable with other highly porous materials and far above than what industrial amine sorbents capture. N<sub>2</sub> uptakes at 273~323 K of the starting material and its derivatives are neither remarkable nor unexpected (Figure 3).

The isosteric heat of adsorption ( $Q_{st}$ ) value, the heat released when CO<sub>2</sub> molecules are adsorbed, between 35–50 kJ mol<sup>-1</sup> is considered optimal, above which recyclability of the adsorbent requires a high amount of energy in CO<sub>2</sub> capture/release cycles.<sup>[5]</sup> Calculated  $Q_{st}$  values are 30.8 and 19.0 kJ mol<sup>-1</sup> (Figure 3f) for the starting materials COP-130 and COP-130-Ac and 25.6, 30.4, 25.6 kJ mol<sup>-1</sup> for COP-130-Ac-EDA, -DETA, and -NH<sub>2</sub>, respectively.  $Q_{st}$  profile of COP-130 shows strong CO<sub>2</sub> concentration dependence that can be seen from a steep decrease in its isotherm as the CO<sub>2</sub> loading increases. This can be attributed

**Table 1.** Detailed porosity, gas uptake, and separation analyses results.

Material	BET [m <sup>2</sup> /g]	BET micro [m <sup>2</sup> /g]	PSD [nm]	Pore vol. [cm <sup>3</sup> /g]	Micro vol. [cm <sup>3</sup> /g]	CO <sub>2</sub> <sup>[a]</sup> [mmol/g]			$Q_{st}$ [kJ/mol]	CO <sub>2</sub> /N <sub>2</sub> selectivity			H <sub>2</sub> uptake <sup>[b]</sup> [mmol/g]	CH <sub>4</sub> uptake <sup>[c]</sup> [mmol/g]	CO <sub>2</sub> /CH <sub>4</sub> selectivity <sup>[d]</sup> 273 K
						273 K	298 K	323 K		273 K	298 K	323 K			
COP-130	1813	457	3.05	1.15	0.47	1.16/ 3.84	0.54/ 2.36	0.25/ 1.38	30.8	45.9	28.0	13.9	7.02	1.25	8.29/7.92
COP-130-Ac	1461	918	2.24	0.64	0.47	1.06/ 4.58	0.71/ 3.83	0.35/ 2.25	19.0	25.1	29.0	13.2	9.59	1.59	4.84/5.04
COP-130-Ac-EDA	1002	744	1.98	0.38	0.33	1.31/ 4.95	0.56/ 2.81	0.27/ 1.64	25.6	27.9	23.4	14.3	9.65	1.52	5.90/6.42
COP-130-Ac-DETA	827	616	1.99	0.31	0.28	1.07/ 3.72	0.44/ 2.09	0.20/ 1.24	30.4	105.7	51.4	30.2	9.02	1.10	8.66/8.46
COP-130-Ac-NH <sub>2</sub>	937	639	2.00	0.38	0.31	1.09/ 4.37	0.46/ 2.45	0.22/ 1.42	25.6	25.5	21.0	12.9	7.03	1.39	5.35/5.69

[a] At 0.15/1 bar; [b] 77 K; [c] 273 K; [d] CO<sub>2</sub>/CH<sub>4</sub> at 5:95 and 50:50.

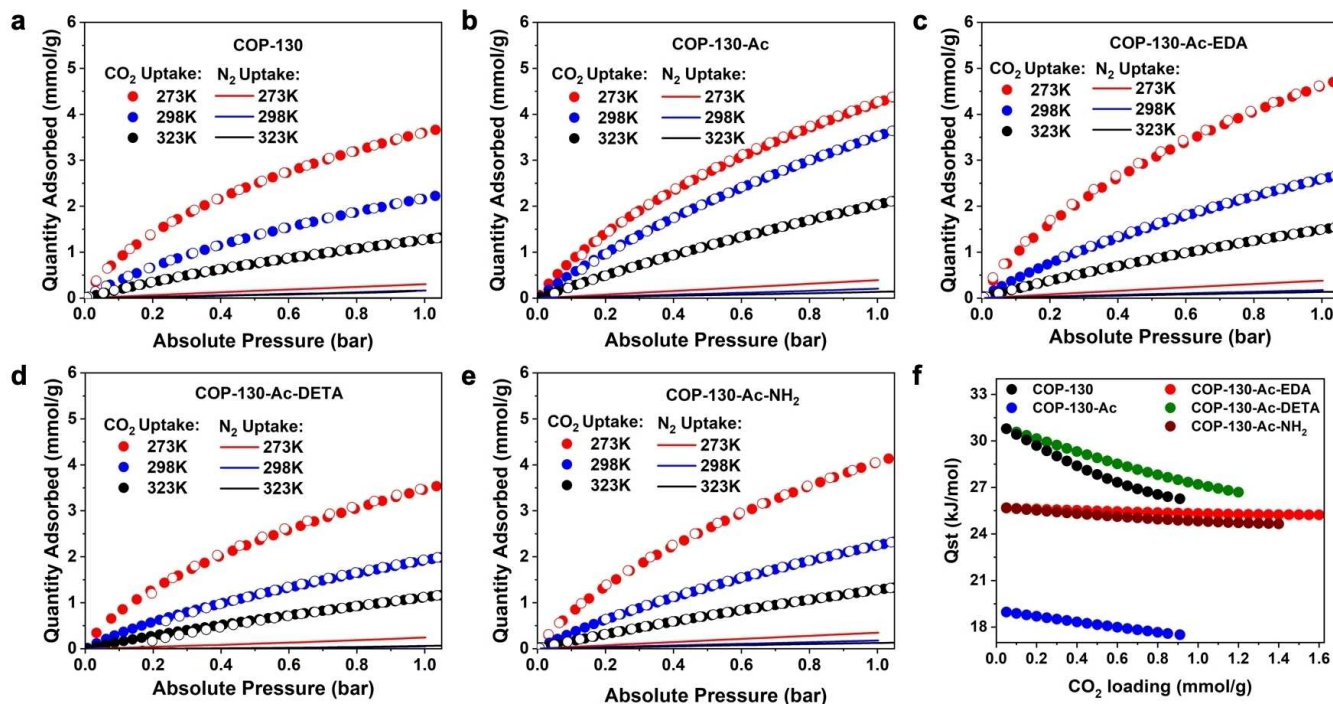


**Figure 3.** CO<sub>2</sub> (dotted) and N<sub>2</sub> (solid lines) uptake at 273 K (red), 298 K (blue), and 323 K (black) of a) COP-130, b) COP-130-Ac, c) COP-130-Ac-EDA, d) COP-130-Ac-DETA, e) COP-130-Ac-NH<sub>2</sub>. f) Q<sub>st</sub> values of COP-130, COP-130-Ac, and COP-130-Ac-Amines.

to the microporosity of the polymer, where contact surface initially covered and the deposition in the subsequent layers quickly lower the adsorption enthalpy. A decrease in Q<sub>st</sub> value in COP-130-Ac can be associated with a twice increase in microporosity that results in a much higher amount of N<sub>2</sub> uptake (Q<sub>st</sub> calculation uses N<sub>2</sub> uptake as a reference inert gas) compared to the increase in CO<sub>2</sub> uptake. The aminated materials have relatively lower heats of adsorption compared to previously reported alkylamine attached porous polymers such as porous aromatic frameworks (PAFs),<sup>[27]</sup> porous polymer networks (PPNs),<sup>[16]</sup> metal organic frameworks (MOFs),<sup>[8,28]</sup> and covalent organic polymers (COPs)<sup>[4c]</sup> that have Q<sub>st</sub> values as high as the conventional MEA solution (50–100 kJ mol<sup>-1</sup>).

Alkylamines, both liquid and attached to porous frameworks, have been widely used as they selectively and chemically bind CO<sub>2</sub> through carbamate formation.<sup>[4c]</sup> However, the strong binding advantage has always taken its toll during the regeneration of sorbents with a high energy penalty that is harmful to materials and financially not feasible in industry. MEA has above 75 kJ mol<sup>-1</sup> heat of adsorption (regeneration energy is equivalent to >120 °C) and most of the reported aminated porous polymers have above 50 kJ mol<sup>-1</sup> (>90 °C) as they tend to capture CO<sub>2</sub> chemisorptively, which means replacing them with conventional amine solutions will not make much difference in terms of energy penalty.<sup>[29]</sup> Therefore, balancing the chemisorption and physisorption of CO<sub>2</sub> by, for example, tuning the amine basicity, is important to achieve high separation and moderate heats of regeneration.<sup>[30]</sup>

Although our aminated materials possess a high amount of amine content and have a noticeable decrease in surface areas

proving that the attached amines are inside the pores-, their CO<sub>2</sub> isotherms do not show any hysteresis, which is a clear indication of minimal chemisorption that happens via an acid-base reaction between CO<sub>2</sub> and the amine groups. In our materials, CO<sub>2</sub> is being adsorbed predominantly via physisorption. The low heats of adsorption of aminated polymers are also in correspondence with physisorptive interaction between CO<sub>2</sub> and amine molecules. One possible reasoning could be ultramicropores being blocked by amines and thus preventing CO<sub>2</sub> from diffusing in and interacting with the rest of the pore volume and the respective amines that are located within the super structure.<sup>[31]</sup> However, this reasoning does not seem to be the most prevalent explanation in this particular case based on two observations. First, if CO<sub>2</sub> molecules are not reaching the amines, we would not observe a 29% increase in total CO<sub>2</sub> uptake while having a 45% loss in the surface area, as that much loss in polymers with no CO<sub>2</sub>-philic moieties would dramatically have decreased the total CO<sub>2</sub> uptake. Second, any pore that can fit a molecule as large as HMTA (which eventually gets broken down to formaldehyde and ammonium chloride salt and leave the pores during intense washing) will easily be able to accommodate CO<sub>2</sub> molecules. So, CO<sub>2</sub> molecules that are diffusing into the polymer are interacting with amines but mostly through physical interaction rather than chemical, which compels us to come up with a more plausible explanation. Whether amines will bind CO<sub>2</sub> chemically or not depends on their basicity strength, that is the charge density of the nitrogen sites. Amines that become less basic due to electron-withdrawing groups will be unable to bind CO<sub>2</sub> covalently and will resort to interact through physical forces. El-Kaderi group

observed this phenomenon after attaching non-alkylated primary amine directly to phenyl rings that eventually rendered amines less basic.<sup>[32]</sup> In most of the reported amine post-modification of porous materials, the substitution of amine molecules with leaving groups (such as alkyl halide, carbonyl, etc.) occurred at the spots that are distantly located. Therefore, the attached amine molecules were located far from each other's reach and couldn't interact with one another. Chloroacetyl chloride has two functional groups, namely C=O and C-Cl, that will accommodate at least two EDA or DETA molecules that will be suitably positioned to establish intramolecular amine-amine hydrogen bond (N-H-N), which in return drain the nitrogen atoms out of electrons and leave them unable to bind strongly to CO<sub>2</sub> molecules.<sup>[17]</sup> COP-130-Ac-NH<sub>2</sub>'s structure also suggests the possibility of the formation of a five-membered ring that includes the N-H-O hydrogen bond, which hinders CO<sub>2</sub> from forming a chemical bond with the amine. This led us to believe that due to the population of amine groups and close proximity of these groups to each other allowed formation of hydrogen bonding, which resulted in broad amine signals in FTIR (Figure 1b) and relatively low heats of adsorption for CO<sub>2</sub> binding. These observations are in line with the works of Danon et al.<sup>[33]</sup> and Hicks et al.<sup>[34]</sup>

CO<sub>2</sub>/N<sub>2</sub> selectivity of a material is as crucial as its total CO<sub>2</sub> uptake capability as post-combustion flue gas streams contain up to 85% N<sub>2</sub>. For almost pure CO<sub>2</sub> production from capture

processes, a sorbent needs to possess at least 100 times more selectivity towards CO<sub>2</sub>. Gas selectivity for CO<sub>2</sub> and N<sub>2</sub> mixture with 15:85 ratio was calculated using ideal adsorbed solution theory (IAST) and is plotted against pressure in Figure 4. COP-130 shows good selectivity, for a polymer that contains of mainly carbon and hydrogen, which reaches up to 45 and rapidly decreases with an increase in temperature and pressure. COP-130-Ac-EDA and -NH<sub>2</sub> also have relatively high N<sub>2</sub> uptake and thus do not show improvement in their respective selectivities, which are 27 and 25. DETA attached polymer has the lowest N<sub>2</sub> uptake and thus demonstrates a significant increase in CO<sub>2</sub>/N<sub>2</sub> selectivity that escalates to 105.

H<sub>2</sub> uptake of COP-130 at 77 K reached 7.02 mmol/g (Figure 5a). Increase in microporous surface area in COP-130-Ac results in even higher H<sub>2</sub> uptake (9.59 mmol/g) with aminated polymers following its lead, -EDA 9.65 mmol/g and -NH<sub>2</sub> 9.02 mmol/g, except for -DETA that decreases to 7.03 mmol/g. In terms of CH<sub>4</sub> uptake, COP-130-Ac has the highest value of 1.59 mmol/g while -DETA has the lowest uptake (1.09 mmol/g) and the rest of the polymers lie in between (Figure 5b). Removal of CO<sub>2</sub> from natural gas, namely "sweetening" process, is crucial for its use as fuel. IAST based method was utilized to test our polymers for CO<sub>2</sub>/CH<sub>4</sub> selectivity (Figure S1). COP-130-Ac-DETA showed the highest uptake for both CO<sub>2</sub>/CH<sub>4</sub> = 05:95 mixture for natural gas sweetening (8.66) and CO<sub>2</sub>/CH<sub>4</sub> = 50:50 mixture for landfill gas purification (8.46). Acylated COP-130

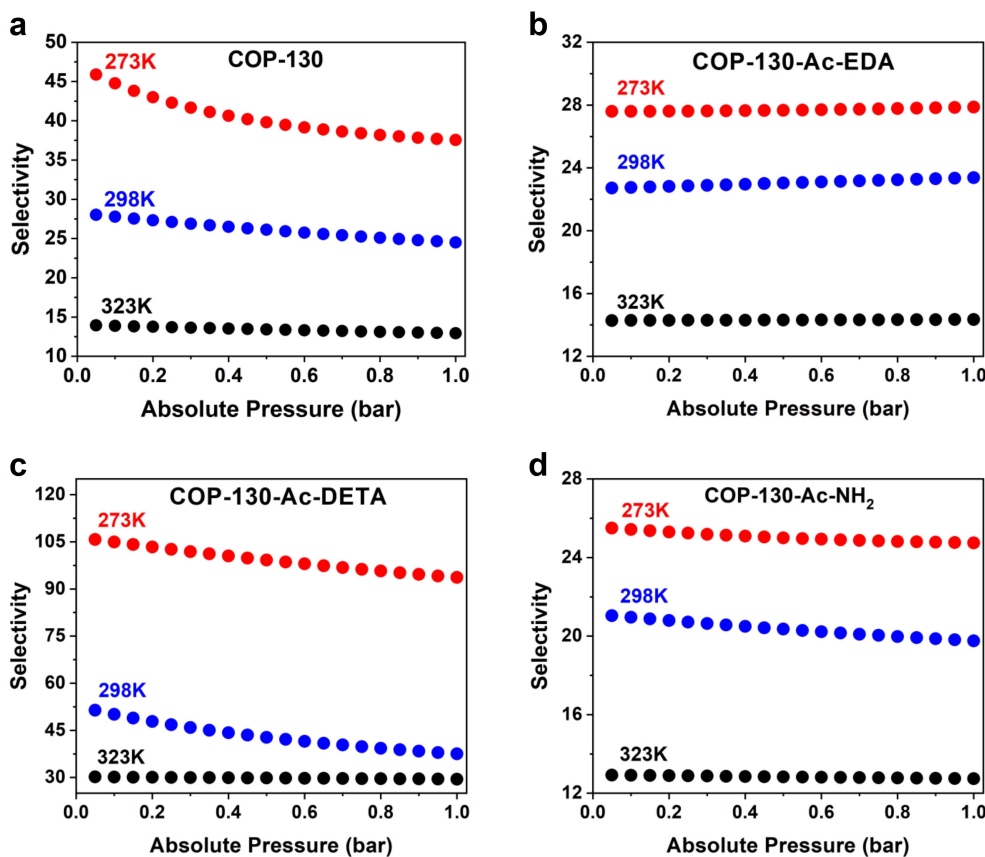


Figure 4. CO<sub>2</sub>/N<sub>2</sub> selectivities at 273 K (red), 298 K (blue), and 323 K (black) of a) COP-130, b) COP-130-Ac-EDA, c) COP-130-Ac-DETA, d) COP-130-Ac-NH<sub>2</sub>.

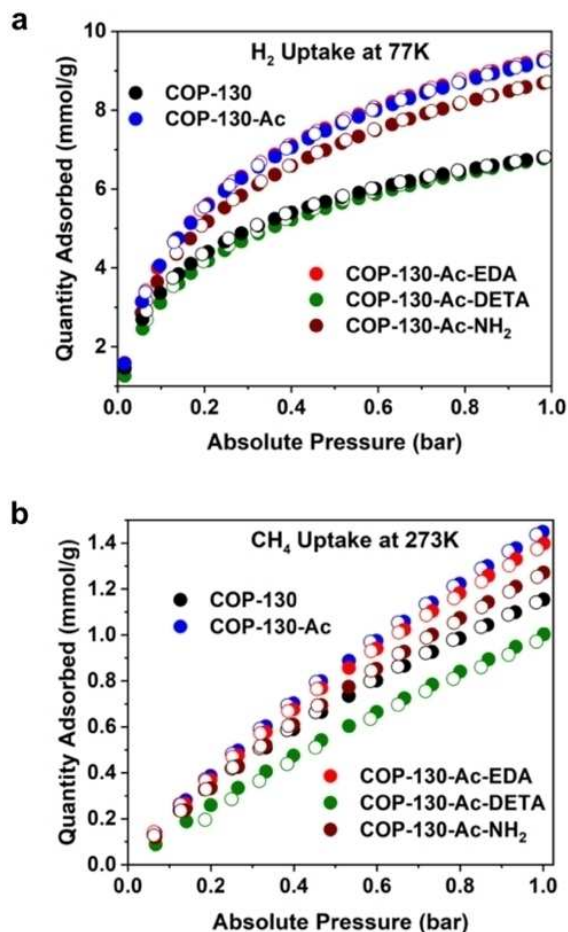


Figure 5. a) H<sub>2</sub> uptake at 77 K, b) CH<sub>4</sub> uptake at 273 K.

showed the lowest selectivity for both gas sweetening (4.84) and purification (5.04) mixtures while all other polymers were found in between. These observations can be explained from COP-130-Ac's highest and -DETA's lowest CH<sub>4</sub> uptake.

## Conclusions

A highly porous polymer is shown to be functionalized without significant surface area loss with amines of varying sizes. The main advantages of the porous polymers reported here were the tethering spots that consist of dual amine substitutable groups with rare ketone functionality. The conventional CO<sub>2</sub> scrubbing methods and most of the aminated sorbents suffer from high regeneration energy penalty. In this work, we managed to significantly increase the CO<sub>2</sub> uptake and selectivity of COP-130 utilizing various amines while maintaining a low isosteric heat of adsorption that is essential for the recyclability of the sorbent. Depositing amine molecules in close proximity to each other allowed the formation of intramolecular hydrogen bonding that hindered the materials from reaching their highest possible CO<sub>2</sub> uptake potential, but in return rewarded the aminated porous polymers with cost-effective heats of

regeneration. When coupled with their overall high CO<sub>2</sub> uptake and selectivity, these findings reinforce the potential of these new materials for industrial applications.

## Experimental Section

### Materials and methods

Dichloromethane (DCM, 99.5%), chloroform (99.5%), methanol (MeOH, 99.0%), ethyl alcohol (EtOH, 99.5%), hexamethylenetetramine (HMTA, 99%), and hydrochloric acid (HCl, 35–37%) were purchased from Samchun Pure Chemicals. 1,3,5-triphenylbenzene (99%) was purchased from Acros Organics. Aluminum chloride (95%) was purchased from Junsei Chemicals. Chloroacetyl chloride (98%) and diethylenetriamine (DETA, 99%) were purchased from Sigma Aldrich. Ethylenediamine (EDA, 99%) was purchased from Alfa Aesar. All the chemicals were utilized as received without further purification. FT-IR spectra were measured by a Perkin-Elmer FTIR spectrometer. To evaluate the porosity and BET surface area ( $P/P_0=0.01-0.25$ ) of COP-130 and derivatives, N<sub>2</sub> adsorption isotherms at 77 K, using liquid nitrogen to ensure the temperature stability, were obtained with a Micromeritics 3Flex surface characterization analyzer, degassing the samples at 120 °C for 10 h under vacuum. The surface area of the samples was calculated by the Brunauer-Emmett-Teller (BET) method. The CO<sub>2</sub> and N<sub>2</sub> adsorption-desorption isotherms for the sorbent were measured at 273, 298, and 323 K by using a static volumetric system (3Flex surface characterization analyzer, Micromeritics Inc.). The adsorption and desorption temperature was kept constant by using a proportional-integral-derivative (PID) controller. Pore size distribution was calculated with the Micromeritics 3FLEX software using a multi-walled carbon nanotube NLDFT model assuming cylindrical pore shape. This model was chosen as it gave the best fit between experiment and calculation. Elemental analysis was performed at the KAIST Central Research Instrument Facility on a Thermo Scientific FLASH 2000 equipped with a TCD detector for carbon, nitrogen, and hydrogen. Each material is measured twice and the elemental composition is given as a mean value of the two measurements. Aluminum content was measured using thermogravimetric analyses (TGA) that were performed on a Shimadzu DTG-60A by heating the polymers to 800 °C at a rate of 5 °C min<sup>-1</sup> under the air atmosphere.

### Synthetic procedures

**Synthesis of COP-130.** 1,3,5-triphenylbenzene (1 g, 3.26 mmol) and dry solid AlCl<sub>3</sub> (1.31 g, 9.82 mmol) are sealed in a 50 mL round bottom flask along with a stirring bar. The flask is flushed thoroughly with N<sub>2</sub> to maintain an inert atmosphere. An excess amount of the linker solvent DCM (20 mL) is injected into the vial and the mixture is heated up to 38 °C and stirred vigorously for 24 h under an inert atmosphere (caution: side product HCl builds up pressure inside the vial). After 24 h, the reaction is stopped and quenched with slow addition of methanol (caution: the reaction of AlCl<sub>3</sub> with methanol is highly exothermic). The precipitate is filtered, washed with methanol and chloroform (10 mL each), and sonicated for an hour in 1 M HCl in methanol to remove leftover AlCl<sub>3</sub> from the pores. To cleanse the polymer from any other contamination, the solid product is washed in a Soxhlet extractor with a 100 mL chloroform and 100 mL methanol mixture for 24 h. The product is dried in a convection oven overnight followed by vacuum drying at 120 °C for 12 h.

**Synthesis of COP-130-Ac.** Post-modification of COP-130 involves Friedel-Crafts acylation with chloroacetyl chloride. 1 g of COP-130 and 2 g of  $\text{AlCl}_3$  are sealed in a 50 mL round bottom flask along with a stirring bar. An excess amount of chloroacetyl chloride (20 mL) is injected into the vial and the mixture is heated up to 50 °C and stirred for 24 h. After the reaction is complete, the mixture is quenched with methanol followed by distilled water (caution: the reaction of  $\text{AlCl}_3$  with methanol and of chloroacetyl chloride with water is highly exothermic). The product is filtered, washed with methanol and chloroform (10 mL each), and sonicated for an hour in 1 M HCl in methanol to remove leftover  $\text{AlCl}_3$ . To cleanse the polymer from any other contamination, the solid product is washed in a Soxhlet extractor with a 100 mL chloroform and 100 mL methanol mixture for 24 h. The product is dried in a convection oven overnight followed by vacuum drying at 110 °C for 12 h. The product is indexed as COP-130-Ac (Ac stands for acylated). See the Supporting Information for the details of the synthetic methods (Scheme S1) and the model compound synthesis (Scheme S3) for the confirmation of the acyl chloride reaction rather than the methyl chloride (Figure S4).

**Synthesis of COP-130-Ac-EDA and -DETA.** Amination of COP-130-Ac with ethylenediamine (EDA) and diethylenetriamine (DETA) is performed by the addition of 0.25 g of COP-130-Ac and 20 mL of liquid amine into a 50 mL round bottom flask with a stirring bar followed by tightly sealing the flask with a rubber septum. The reaction is brought to 80 °C and stirred for 24 h. After the reaction is complete, the mixture is quenched with distilled water, and the product is filtered, washed with 100 mL distilled water, 100 mL methanol, and 100 mL chloroform and dried in a convection oven overnight followed by vacuum drying at 110 °C for 12 h.

**Synthesis of COP-130-Ac-HMTA and -NH<sub>2</sub>.** Amination of COP-130-Ac with solid HMTA is performed by the addition of 0.25 g of COP-130-Ac and 2 g of HMTA followed by injection of 20 mL solvent ethanol into a 50 mL round bottom flask and the mixture is stirred at 80 °C for 24 h. After the reaction is complete, the product is collected by filtration, washed with 100 mL distilled water, 100 mL methanol, and 100 mL chloroform and dried in a convection oven overnight followed by vacuum drying at 110 °C for 12 h. After complete drying, all of COP-130-Ac-HMTA is reacted with 2 M HCl in 20 mL solvent ethanol in a 50 mL round bottom flask at 80 °C for 24 h. The product, COP-130-Ac-NH<sub>2</sub>, undergoes the same washing and drying procedure as its predecessor -HMTA. The reaction of HMTA with COP-130-Ac (and the following acid treatment) occurs via the Delépine mechanism according to which HMTA substitutes the Cl atoms of the acetyl chloride group and forms quaternary ammonium chloride salt. Further treatment with strong acid converts the attached HMTA ring into a primary amine.

## Acknowledgements

This research was supported by KAIST Institute for NanoCentury (KINC 2020).

## Conflict of Interest

The authors declare no conflict of interest.

**Keywords:** amine impregnation · carbon capture · Friedel-Crafts acylation · nanoporous materials · post-modification

- [1] D. Lüthi, M. Le Floch, B. Bereiter, T. Blunier, J.-M. Barnola, U. Siegenthaler, D. Raynaud, J. Jouzel, H. Fischer, K. Kawamura, T. F. Stocker, *Nature* **2008**, *453*, 379–382.
- [2] Global Monitoring Laboratory, Earth System Research Laboratories, **2020**, September 9.
- [3] D. Y. C. Leung, G. Caramanna, M. M. Maroto-Valer, *Renewable Sustainable Energy Rev.* **2014**, *39*, 426–443.
- [4] a) K. Sumida, D. L. Rogow, J. A. Mason, T. M. McDonald, E. D. Bloch, Z. R. Herm, T.-H. Bae, J. R. Long, *Chem. Rev.* **2012**, *112*, 724–781; b) E. E. Ünveren, B. Ö. Monkul, Ş. Sariođlan, N. Karademir, E. Alper, *Petroleum* **2017**, *3*, 37–50; c) D. Thirion, V. Rozyyev, J. Park, J. Byun, Y. Jung, M. Atilhan, C. T. Yavuz, *Phys. Chem. Chem. Phys.* **2016**, *18*, 14177–14181; d) J. Wang, L. Huang, R. Yang, Z. Zhang, J. Wu, Y. Gao, Q. Wang, D. O'Hare, Z. Zhong, *Energy Environ. Sci.* **2014**, *7*, 3478–3518.
- [5] H. A. Patel, J. Byun, C. T. Yavuz, *ChemSusChem* **2017**, *10*, 1303–1317.
- [6] a) T. O. Nelson, A. Kataria, P. Mobley, M. Soukri, J. Tanthana, *Energy Procedia* **2017**, *114*, 2506–2524; b) O. Buyukcakir, S. H. Je, J. Park, H. A. Patel, Y. Jung, C. T. Yavuz, A. Coskun, *Chem. Eur. J.* **2015**, *21*, 15320–15327; c) W. Zhang, F. Ma, L. Ma, Y. Zhou, J. Wang, *ChemSusChem* **2020**, *13*, 341–350.
- [7] a) E. Jang, S. W. Choi, S.-M. Hong, S. Shin, K. B. Lee, *Appl. Surf. Sci.* **2018**, *429*, 62–71; b) G. Singh, K. S. Lakhi, K. Ramadass, C. I. Sathish, A. Vinu, *ACS Sustainable Chem. Eng.* **2019**, *7*, 7412–7420.
- [8] T. M. McDonald, W. R. Lee, J. A. Mason, B. M. Wiers, C. S. Hong, J. R. Long, *J. Am. Chem. Soc.* **2012**, *134*, 7056–7065.
- [9] a) V. Guillemin, Ł. J. Weseliński, M. Alkordi, M. I. H. Mohideen, Y. Belmabkhout, A. J. Cairns, M. Eddaoudi, *Chem. Commun.* **2014**, *50*, 1937–1940; b) H. A. Patel, C. T. Yavuz, *Faraday Discuss.* **2015**, *183*, 401–412; c) N. A. Dogan, Y. Hong, E. Ozdemir, C. T. Yavuz, *ACS Sustainable Chem. Eng.* **2019**, *7*, 123–128.
- [10] T. S. Nguyen, C. T. Yavuz, *Chem. Commun.* **2020**, *56*, 4273–4275.
- [11] V. Rozyyev, D. Thirion, R. Ullah, J. Lee, M. Jung, H. Oh, M. Atilhan, C. T. Yavuz, *Nat. Energy* **2019**, *4*, 604–611.
- [12] a) J. Byun, H. A. Patel, D. Thirion, C. T. Yavuz, *Nat. Commun.* **2016**, *7*, 13377; b) J. Byun, H. A. Patel, D. Thirion, C. T. Yavuz, *Polymer* **2017**, *126*, 308–313; c) Y. Hong, D. Thirion, S. Subramanian, M. Yoo, H. Choi, H. Y. Kim, J. F. Stoddart, C. T. Yavuz, *Proc. Natl. Acad. Sci. USA* **2020**, *117*, 16174.
- [13] a) S. Subramanian, J. Oppenheim, D. Kim, T. S. Nguyen, W. M. H. Silo, B. Kim, W. A. Goddard III, C. T. Yavuz, *Chem* **2019**, *5*, 3232–3242; b) C. Cao, D.-D. Ma, J.-F. Gu, X. Xie, G. Zeng, X. Li, S.-G. Han, Q.-L. Zhu, X.-T. Wu, Q. Xu, *Angew. Chem. Int. Ed.* **2020**, *59*, 15014–15020; *Angew. Chem.* **2020**, *132*, 15124–15130; c) H. Chen, Z. Yang, C.-L. Do-Thanh, S. Dai, *ChemSusChem* **2020**, *13*, DOI: 10.1002/cssc.202001638; d) S. Subramanian, Y. Song, D. Kim, C. T. Yavuz, *ACS Energy Lett.* **2020**, *5*, 1689–1700; e) Y.-L. Zheng, H.-C. Liu, Y.-W. Zhang, *ChemSusChem* **2020**, *13*, DOI: 10.1002/cssc.202001290.
- [14] N. A. Dogan, E. Ozdemir, C. T. Yavuz, *ChemSusChem* **2017**, *10*, 2130–2134.
- [15] J. Byun, D. Thirion, C. T. Yavuz, *Beilstein J. Nanotechnol.* **2019**, *10*, 1844–1850.
- [16] W. Lu, M. Bosch, D. Yuan, H.-C. Zhou, *ChemSusChem* **2015**, *8*, 433–438.
- [17] A. Danon, P. C. Stair, E. Weitz, *J. Phys. Chem. C* **2011**, *115*, 11540–11549.
- [18] M. Arockia doss, G. Rajarajan, E. Dhineshkumar, S. Amala, V. Thanikachalam, S. Selvanayagam, B. Sridhar, *J. Mol. Struct.* **2020**, *1200*, 127076.
- [19] G. Socrates, *Infrared and Raman characteristic group frequencies: tables and charts*, 3rd ed., Wiley, **2004**.
- [20] X. Wang, J. He, J. Huang, *J. Chem. Thermodyn.* **2019**, *131*, 1–8.
- [21] R. Muhammad, P. Rekha, P. Mohanty, *RSC Adv.* **2016**, *6*, 17100–17105.
- [22] a) R. W. Layer, *Chem. Rev.* **1963**, *63*, 489–510; b) M. G. Schwab, B. Fassbender, H. W. Spiess, A. Thomas, X. Feng, K. Müllen, *J. Am. Chem. Soc.* **2009**, *131*, 7216–7217.
- [23] B. Kuhn, P. Mohr, M. Stahl, *J. Med. Chem.* **2010**, *53*, 2601–2611.
- [24] W. Lu, J. P. Sculley, D. Yuan, R. Krishna, Z. Wei, H.-C. Zhou, *Angew. Chem. Int. Ed.* **2012**, *51*, 7480–7484; *Angew. Chem.* **2012**, *124*, 7598–7602.
- [25] C. H. Lau, X. Mulet, K. Konstas, C. M. Doherty, M.-A. Sani, F. Separovic, M. R. Hill, C. D. Wood, *Angew. Chem. Int. Ed.* **2016**, *55*, 1998–2001; *Angew. Chem.* **2016**, *128*, 2038–2041.
- [26] F. Liu, S. Chen, Y. Gao, Y. Xie, *J. Appl. Polym. Sci.* **2017**, *134*, 45046.
- [27] S. J. Garibay, M. H. Weston, J. E. Mondloch, Y. J. Colón, O. K. Farha, J. T. Hupp, S. T. Nguyen, *CrystEngComm* **2013**, *15*, 1515–1519.
- [28] a) U. Jeong, N. A. Dogan, M. Garai, T. S. Nguyen, J. F. Stoddart, C. T. Yavuz, *J. Am. Chem. Soc.* **2019**, *141*, 12182–12186; b) F. Zhang, J. Zhang, B. Zhang, L. Zheng, X. Cheng, Q. Wan, B. Han, J. Zhang, *Nat. Commun.* **2020**, *11*, 1431.



- [29] S. Mukherjee, A. Kumar, M. J. Zaworotko, in *Metal-Organic Frameworks (MOFs) for Environmental Applications* (Ed.: S. K. Ghosh), Elsevier, **2019**, pp. 5–61.
- [30] C. Xu, G. Yu, J. Yuan, M. Strømme, N. Hedin, *Mater. Today* **2020**, *6*, 100052.
- [31] W. Lu, J. P. Sculley, D. Yuan, R. Krishna, Z. Wei, H.-C. Zhou, *Angew. Chem. Int. Ed.* **2012**, *51*, 7480–7484; *Angew. Chem.* **2012**, *124*, 7598–7602.
- [32] T. İslamoğlu, M. Gulam Rabbani, H. M. El-Kaderi, *J. Mater. Chem. A* **2013**, *1*, 10259–10266.
- [33] A. Danon, P. C. Stair, E. Weitz, *J. Phys. Chem. C* **2011**, *115*, 11540–11549.
- [34] J. C. Hicks, R. Dabestani, A. C. Buchanan, C. W. Jones, *Chem. Mater.* **2006**, *18*, 5022–5032.

---

Manuscript received: September 15, 2020  
Revised manuscript received: October 11, 2020  
Accepted manuscript online: October 15, 2020  
Version of record online: October 27, 2020

---